Forest Chemicals Review
www.forestchemicalsreview.com
ISSN: 1520-0191
July-August 2022 Page No. 1592-1607
Article History: Received: 30 March 2022, Revised: 8 April 2022, Accepted: 15 April 2022, Publication: 30 April 2022

Research on UAV Line Inspection System of Transmission Line Electrical Automation Technology

Juanjuan Wang [*], Yanan Wang
Xi'an Traffic Engineering Institute, Xi'an,710300, China.
*Corresponding Author.

Abstract:

Electric power transmission lines have a wide coverage area, complex terrain and harsh natural environment. The line foundation, towers, ground wires, and hardware are violated by the outside world, resulting in defects and hidden dangers. This can easily lead to line failures. This seriously threatens the safety and stable operation of the power grid. In view of the low degree of automation of manual operation of unmanned aerial vehicles for transmission line inspection at present, and the difficulty of standardization and standardization of manual operation of unmanned aerial vehicles, resulting in long line inspection time or multiple crashes, the unmanned aerial vehicle proposed by China Southern Power Grid Corporation has no problem. Humans control the autonomous line inspection targets, and develop an intelligent inspection method for transmission line multi-rotor UAVs based on carrier phase differential positioning technology.

Keywords*: Transmission Line; Electrical Automation; Drone Line Inspection; Intelligent Inspection; Smart Grid*

I. INTRODUCTION

There are many distribution points and wide areas of transmission lines, and many lines are located in the wilderness and the terrain is complex. Regular inspection and maintenance are required to ensure the safety of transmission lines. In recent years, the workload of transmission line inspection has increased sharply with the increase of power grid scale and voltage level and the rapid expansion of long-distance transmission lines. Traditional manual inspection has been difficult to meet the requirements of transmission line inspection [1]. Civilian multi-rotor UAVs are not restricted by terrain. Not only can high-precision aerial photography equipment be used to capture line images along the line, but they can also hover around transmission towers to capture high-precision images and infrared and ultraviolet images from different perspectives to achieve refined line inspections. , has outstanding advantages such as high efficiency, reliability, safety and low cost, can detect hidden dangers in time, reduce labor intensity and risk of climbing towers, and has rapidly developed into an important way of power transmission line inspection.

Forest Chemicals Review
www.forestchemicalsreview.com
ISSN: 1520-0191
July-August 2022 Page No. 1592-1607
Article History: Received: 30 March 2022, Revised: 8 April 2022, Accepted: 15 April 2022, Publication: 30 April 2022

In the process of cruising aerial photography, the shooting position and height of the UAV depend on the artificial visual judgment of the flight controller, and the flight control is heavily dependent on the individual flight control level of the flight controller. Defects, significantly reduce the inspection efficiency. In the process of promoting the application of UAV line inspection, problems such as the difficulty of training a large number of high-level UAV flight controllers have also been exposed [2]. In order to improve the intelligence level of transmission line inspection, it is necessary to realize the standardization and standardization of UAV inspection. To this end, the power grid company has formulated a development plan for UAV intelligent inspection, requiring the realization of unmanned UAV autonomous inspection by 2025.

Under the background of intelligent inspection, the inspection method of UAV with LiDAR, infrared, visible light camera and other sensor technologies has gradually been derived. Among them, the inspection method using consumer-grade drones equipped with visible light cameras is highly intelligent, and has a lower hardware entry threshold and capital cost, and has gradually become popular in provincial power grid inspection departments in various places [3]. In the field of consumer drones, rotorcraft is the backbone of intelligent inspection. Compared with consumer fixed-wing drones, multi-rotor drones are used by various power grids because of their convenience, ease of use, safety and reliability. The company purchases widely.

However, at the beginning of the design, this type of consumer drone is positioned to meet the needs of ordinary aerial photography. Its flight control system is relatively simple, and it often cannot meet the needs of intelligent operations when applied in professional fields [4]. Scenarios are custom developed using SDK tools. Different from normal drone flight, in the inspection operation of the power industry, because the lines are distributed in strips and fluctuate with the terrain, the flying height of the drone, the degree of photo overlap, the imaging resolution, and the route design All have special requirements, so relying on the SDK platform, customized development of a suitable, stable and efficient flight control system can truly meet the needs of intelligent inspection in the power industry.

II. POWER LINE PATROL FLIGHT CONTROL SYSTEM

The electric line patrol flight control system is a flight control software customized for the line patrol requirements of UAVs. Through simple and reasonable route design, the purpose of automatic or semi-automatic operation of supporting UAVs can be achieved [5]. The technical process is as follows: As shown in Figure 1 (the picture is quoted from Software-defined network-enabled opportunistic offloading and charging scheme in multi-unmanned aerial vehicle ecosystem).

Forest Chemicals Review
www.forestchemicalsreview.com
ISSN: 1520-0191
July-August 2022 Page No. 1592-1607
Article History: Received: 30 March 2022, Revised: 8 April 2022, Accepted: 15 April 2022, Publication: 30 April 2022

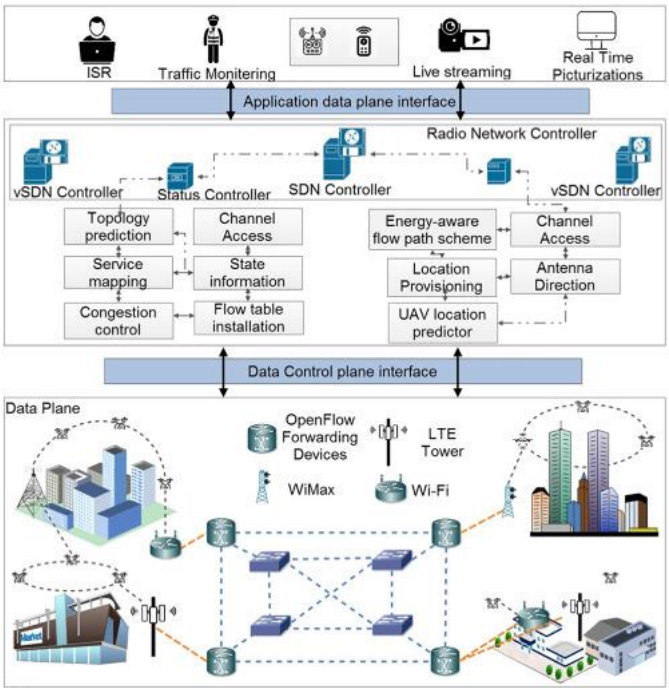

Fig.1 The flow chart of the UAV flight control system in the detection of tree obstacles in power line inspection

Figure 1 describes the working principle and specific process of the power line patrol flight control system. First enter the coordinates of the tower, then set parameters such as flight height and photo overlap, select the head and tail towers that need to perform the line patrol task, then upload the task and wait for the UAV to load, click Start task to make the UAV start fully automatic flight , the flight status can be monitored throughout the flight, waiting for the drone to return and land, and the mission is completed.

2.1. Multi-source data acquisition system

UAV mid- and low-altitude data acquisition technology, as an important means of spatial data acquisition, has the advantages of long battery life, low flight cost, high data resolution, flexible scheduling, etc. It can realize real-time data transmission and can enter high-risk areas. Detection is a powerful supplement to satellite remote sensing and traditional aerial photogrammetry, and has formed a situation of vigorous development in parallel with satellite remote sensing and ordinary aerial remote sensing abroad. Especially in the case of emergency response to major natural disasters, low-altitude optical image acquisition in cloudy weather, timely remote sensing in local areas, low-altitude large-scale high-precision mapping and distributed daily low-altitude remote sensing monitoring, etc. the UAV aerial remote sensing system has satellite remote sensing and ordinary aviation remote sensing. The irreplaceable role of remote sensing [6]. The application of UAV to power line inspection and safety status evaluation of power facilities can make full use of its advantages in cost, timeliness and other aspects, and solve various problems existing in the current use of manual methods.

Forest Chemicals Review
www.forestchemicalsreview.com
ISSN: 1520-0191
July-August 2022 Page No. 1592-1607
Article History: Received: 30 March 2022, Revised: 8 April 2022, Accepted: 15 April 2022, Publication: 30 April 2022

In traditional helicopter patrols, sensors such as infrared thermal imagers and visible light cameras are often used to collect data through manual operations. The acquired data is relatively independent, and each data frame does not have clear location information, and there is no correlation between sensor data, which is difficult to achieve. Unified data management and multi-source data comparative analysis and other applications [7]. The sampling frequency, time reference and time accuracy of various sensor data carried on the unmanned helicopter platform are different, and the original data collected by each sensor are in different coordinate reference systems, so it is difficult for the output data to be in the same time and space reference. on the management. To perform fusion diagnosis, processing and analysis on the data collected by each sensor, it is necessary to solve the problems of time reference and space reference. This paper proposes a method that uses GPS time as the time reference, and unifies the space-time reference of each sensor through the method of synchronous timing, so as to realize the synchronous acquisition of POS data, image and infrared, ultraviolet video stream data, point cloud data and other types of data, and unify the data of each sensor. Time and space benchmarks. The specific synchronization process is shown in Figure 2 (the picture is quoted in A review on drones controlled in real-time).

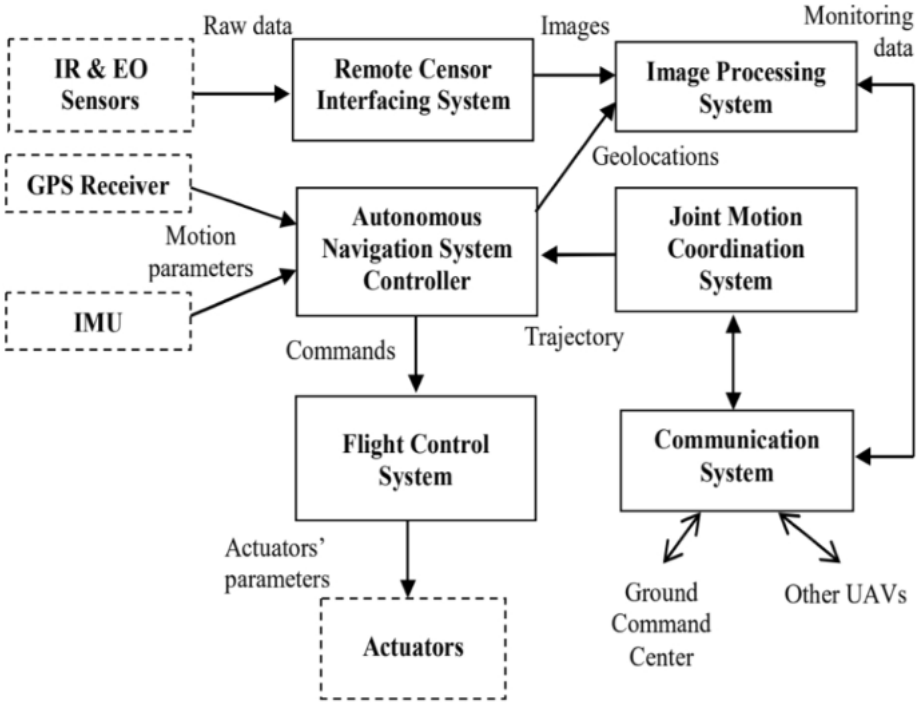

Fig. 2 Unmanned helicopter multi-sensor data acquisition system

The spatial reference for the multi-source data collected by the multi-sensor comes from the attitude sensor-POS system. In this paper, the laser, infrared and ultraviolet sensors are designed to be associated with the POS system. Through the establishment of the unified time coordinates of the airborne sensors, the unification of the time and space benchmarks of the data collected by each sensor is realized. Since programming in high-level computer language cannot record μs or ns-level time with high accuracy, this paper designs a time-serving GPS and a time synchronization controller to realize the synchronous recording of each sensor data, and completes synchronous data acquisition while determining the time

Forest Chemicals Review
www.forestchemicalsreview.com
ISSN: 1520-0191
July-August 2022 Page No. 1592-1607
Article History: Received: 30 March 2022, Revised: 8 April 2022, Accepted: 15 April 2022, Publication: 30 April 2022

reference with high precision, reducing the need for It reduces the task load of the airborne industrial computer and ensures the robustness of the system [8]. The specific implementation is as follows: First, the time signal and pulse-per-second (PPS) signal output by the GPS are introduced into the time synchronization controller, and the time synchronization controller is time-synchronized. The synchronization controller first provides timing to the laser scanner, infrared thermal imager, ultraviolet camera, and visible light camera. After each sensor receives the PPS signal, the second count is reset to zero, so as to obtain the time accurate to μs. The synchronization controller is also used to trigger the camera exposure and send the exposure time to the computer for recording. Through the above steps, the time of POS, visible light camera, laser scanner, infrared thermal imager, and ultraviolet camera data is all unified GPS time, so as to achieve the purpose of unified time reference for multiple data sources. After the time reference is unified, the spatial position and attitude data corresponding to each frame of data collection time of each sensor can be obtained from the raw data recorded by the POS at high frequency (100~200Hz), thus completing the unified spatial reference.

2.2. Flight path

Overhead transmission lines are usually distributed in strips, and drones should fly in strips along overhead transmission lines and towers. If only considering the restoration of the three-dimensional point cloud of the transmission line corridor, it can be completed by using a single-airline flight and matching the dense point cloud through the stereo image pair in the air belt. Carry out forward intersection measurement of the power line. Since the camera takes pictures along the power line during flight, the broad side of the camera is approximately perpendicular to the power line. At this time, if the stereo pair selects adjacent images in the route, the power line cannot be accurately selected by adjusting the left and right parallax. Therefore, the power line vector cannot be accurately extracted [9]. At this time, another route needs to be laid to ensure a certain degree of overlap between the two routes. The stereo pair selects the adjacent images between the routes. By adjusting the left and right parallax, the image point of the same name on the power line can be accurately selected, and the power line vector can be accurately extracted. Take a span as an example: two routes are designed along the direction of the power line, and are laid on the left and right sides directly above the two towers. The drone takes off from the vicinity of the first tower to above the tower, starts to fly along one wire to the second tower, and then returns to the take-off point along the other wire to land.

2.3. Data Visualization Methods

The massive cloud data of laser point is the basic data source of the visualization system of transmission line corridor. Through the laser point cloud data, the terrain data of the target scene can be quickly generated, and the tower/transmission line model and other terrain can be extracted from it. The ability to schedule laser point cloud data smoothly and quickly is the primary task of processing laser point cloud data. The 3D data of terrain environment includes digital orthophoto (DOM) and digital elevation model (DEM), which is a rasterized 3D representation of the real environment. At present, the management and real-time visualization of laser point massive cloud data and terrain data are still the key issues in virtual geographic environment [10]. The solution to realize visualization needs to meet the

Forest Chemicals Review
www.forestchemicalsreview.com
ISSN: 1520-0191
July-August 2022 Page No. 1592-1607
Article History: Received: 30 March 2022, Revised: 8 April 2022, Accepted: 15 April 2022, Publication: 30 April 2022

requirements of users to smoothly visualize 3D laser point cloud data and terrain data in the computer or network environment. One of the difficulties is how to overcome the limited storage space of the computer. Therefore, this paper establishes a level of detail model (LOD), and uses the regional quadtree space and quadtree data index to dynamically schedule the data within the field of view, so as to realize the real-time visualization of the massive cloud data and terrain data of laser points.

2.4. Real-time 3D visualization method

The visualization of the tower/transmission line model is a key part of the transmission line corridor visualization system. There are many types of tower models, their data is very complex, and the relationship between points is also complicated. The type of tower also determines the number and spatial distribution of transmission lines. Therefore, how to visualize the tower/transmission line model is the key to efficient, smooth, multi-perspective and realistic visualization of the line corridor. In order to truly reflect the three-dimensional structure of the iron tower, the fine modeling of the iron tower requires the tower drawings as the basic data. The operator sets the specifications according to the drawings and uses professional modeling software such as 3DMax to build the three-dimensional model of the iron tower. In this paper, the position of the tower is measured from the laser point cloud data for model insertion. Extract and fit the power line laser point cloud data for 3D laser scanning to obtain the power line vector model. For long-distance high-voltage transmission lines, transmission line corridors can reach hundreds or thousands of kilometers, and there are many towers. To solve this problem, the subsystem design of the tower/transmission line model still uses the LOD technology to display the tower model in layers, and displays the tower model with different levels of detail at different scales to achieve a balance between high-efficiency processing and high-effect vision. The design of the tower/transmission line model visualization subsystem adopts the method of real-time dynamic calling and pre-established LOD tower model that meets the specifications, and then displays it to the given tower coordinate position to realize the visualization of the tower, and import the extracted transmission line model, so as to realize 3D visualization of the complete line corridor. The real-time 3D visualization subsystem of the unmanned helicopter flight process realistically reproduces the flight position and attitude information of the unmanned helicopter in the pre-established transmission line corridor environment data in a true 3D form, as well as the transmission line corridor environment during the flight [11]. The visualization of terrain data and tower/transmission line models is the premise of simulating the flight environment of unmanned helicopters. The virtual line corridor environment is constructed using the real-time 3D visualization technology of terrain. In this environment, according to the track data recorded by the flight control system during the line patrol process, the virtual flight of the unmanned helicopter line patrol can be realized, the real scene of the power line corridor can be reproduced, and the status of the tower/power line can be judged by the inspectors. Accurate and fast information.

Forest Chemicals Review
www.forestchemicalsreview.com
ISSN: 1520-0191
July-August 2022 Page No. 1592-1607
Article History: Received: 30 March 2022, Revised: 8 April 2022, Accepted: 15 April 2022, Publication: 30 April 2022

III. BASIC MATHEMATICAL MODEL OF TRADITIONAL QUADROTOR UAV

3.1. Kinetic equation

The range of motion of the aircraft itself is in the space coordinate system, and its degrees of freedom have uncontrollable factors, so generally do not limit its degrees of freedom to maintain its six degrees of freedom in space, namely $(\mathrm{x},\mathrm{y},\mathrm{z},\theta,\phi,\psi)$. Among them, (x,y,z) represents the specific position of the three-dimensional coordinates of the drone in space, and (θ,φ,ψ) represents the angle between the drone itself and the x, y, and z axes of the coordinate axis. The coordinate system established on the body of the quadcopter is called the body coordinate system $(OX_BY_BZ_B)$, as shown in Figure 3(a), the origin of the body coordinate system must be guaranteed to coincide with the center of mass of the body. The O_BX_B axis is parallel to the straight line where the motors M1 and M3 are located, and the positive direction is the M1 direction. The O_BY_B axis is parallel to the straight line where the motors M2 and M4 are located, and the positive direction is the direction of the motor M2. The O_BZ_B axis is perpendicular to the plane where the O_BX_B and O_BY_B axes lie. The changes of the attitude angle and three-dimensional position coordinates of the quadrotor UAV refer to a certain point on the ground, so a reference coordinate system must be built on the ground, that is, the ground coordinate system （$OX_EY_EZ_E$）, as shown in Figure 3(b).

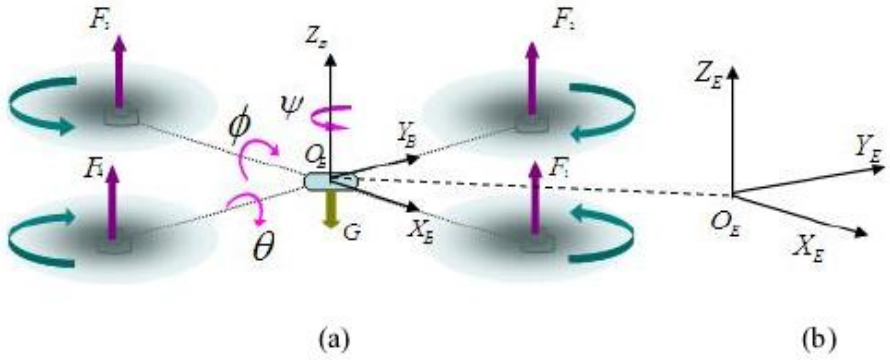

Fig. 3 Quadcopter coordinate system

Because the ground coordinates and the fuselage coordinates need to be calculated between the two, Euler angles are introduced to analyze the relationship between the two to solve the calculation problem of air attitude and position for the convenience of calculation and analysis. The roll angle ϕ is the angle between the O_BY_B axis in the body coordinate system and the $O_EX_EY_E$ plane of the ground coordinate system; the pitch angle θ is the angle between the O_BX_B axis in the body coordinate system and the $O_EX_EY_E$ plane of the ground coordinate system; the heading angle ψ is the body coordinate system. The projection line of the O_BX_B axis on the $O_EX_EY_E$ plane of the ground coordinate system, and the included angle of the O_EX_E axis. From the above definition, it can be concluded that the conversion equations from the coordinate system of the four-axis UAV body to each axis of the geodetic coordinate

Forest Chemicals Review
www.forestchemicalsreview.com
ISSN: 1520-0191
July-August 2022 Page No. 1592-1607
Article History: Received: 30 March 2022, Revised: 8 April 2022, Accepted: 15 April 2022, Publication: 30 April 2022

system are respectively expressed as formula (1):

$$\begin{aligned} \mathrm{R}_{\phi} &= \begin{pmatrix} 1 & 0 & 0 \\ 0 & \cos\phi & -\sin\phi \\ 0 & \sin\phi & \cos\phi \end{pmatrix} \\ \mathrm{R}_{\theta} &= \begin{pmatrix} \cos\theta & 0 & \sin\theta \\ 0 & 1 & 0 \\ -\sin\theta & 0 & \cos\phi \end{pmatrix} \\ \mathrm{R}_{\phi} &= \begin{pmatrix} \cos\psi & -\sin\psi & 0 \\ \sin\psi & \cos\phi & 0 \\ 0 & 0 & 1 \end{pmatrix} \end{aligned} \tag{1}$$

It can be known that the transformation matrix from the body coordinate system B to the ground coordinate system E is:

$$\mathrm{R}_{EtoB} = \mathrm{R}_{\phi}\mathrm{R}_{\theta}\mathrm{R}_{\psi}$$

$$\mathrm{R}_{EtoB} = \begin{pmatrix} \cos\psi\cos\phi & \cos\psi\sin\theta\sin\phi & \cos\psi\sin\theta\cos\phi+\sin\psi\sin\phi \\ \sin\psi\cos\theta & \sin\psi\sin\theta\sin\phi & \sin\psi\sin\theta\cos\phi-\sin\phi\cos\psi \\ -\sin\theta & \cos\theta\sin\phi & \cos\theta\cos\phi \end{pmatrix} \tag{2}$$

Among them, $\mathbf{R}_{EtoB}$ is the space coordinate system transformation relationship between the quadrotor aircraft fuselage center of mass coordinate system and the stationary geodetic coordinate system [12]. The following paper deduces the model of the aircraft from linear motion and angular motion. The linear motion changes the rotational speed of the four motors of the quadrotor, and the force on the aircraft will change, resulting in the acceleration of the linear motion.

$$\begin{aligned} G &= \mathrm{mg} \\ \mathrm{F_i} &= \frac{1}{2}\rho \mathrm{C_i}\omega_i^2 = k_i\omega_i^2 \\ D_i &= \frac{1}{2}\rho \mathrm{C_d}\omega_i^2 = k_d\omega_i^2 \end{aligned} \tag{3}$$

Among them, G is the gravity of the aircraft, F_{i}, $\mathrm{i}=1,2,3,4$ is the lift generated by the i rotor, D_{i} is the resistance of the i rotor, C_{t} is the lift parameter of the rotor, C_{d} is the drag parameter of the rotor, and ω_{i} is the i rotor. $\mathrm{k_t}$ is the lift coefficient, and $\mathrm{k_d}$ is the drag coefficient. According to the force analysis of the quadrotor aircraft in Figure (3), and applying Newton's laws of mechanics, the translational dynamic model relative to the earth coordinate system is obtained as:

Forest Chemicals Review
www.forestchemicalsreview.com
ISSN: 1520-0191
July-August 2022 Page No. 1592-1607
Article History: Received: 30 March 2022, Revised: 8 April 2022, Accepted: 15 April 2022, Publication: 30 April 2022

$$m\ddot{\xi} = F_f - k_{dt}\dot{\xi} - mg \tag{4}$$

Among them, is the mass of the quadrotor helicopter, $\xi\xi = (x, y, z)^T$ is the translation position of the helicopter, $\mathbf{g} = (0,0,g)^T$ is the gravitational acceleration, k_{dt} is the translational drag coefficient, and $\mathbf{F}_f = (F_x, F_y, F_z)^T$ is the total lift of the four propellers of the helicopter.

$$F = R_{EtoB}\begin{pmatrix} 0 \\ 0 \\ \sum_{i=1}^{4} F_i \end{pmatrix} = \begin{pmatrix} \cos\phi\cos\theta\sin\psi + \sin\phi\sin\psi \\ \cos\phi\sin\psi\sin\theta - \sin\phi\cos\psi \\ \cos\phi\cos\theta \end{pmatrix} \sum_{i=1}^{4} F_i \tag{5}$$

We substitute equation (5) into equation (4) to get

$$m\begin{pmatrix} \ddot{x} \\ \ddot{y} \\ \ddot{z} \end{pmatrix} = \begin{pmatrix} \cos\phi\cos\theta\sin\psi + \sin\phi\sin\psi \\ \cos\phi\sin\psi\sin\theta - \sin\phi\cos\psi \\ \cos\phi\cos\theta \end{pmatrix} \sum_{i=1}^{4} F_i - \begin{pmatrix} k_{dtx} & 0 & 0 \\ 0 & k_{dty} & 0 \\ 0 & 0 & k_{dtz} \end{pmatrix} \begin{pmatrix} \dot{x} \\ \dot{y} \\ \dot{z} \end{pmatrix} - m\begin{pmatrix} 0 \\ 0 \\ g \end{pmatrix} \tag{6}$$

Sorted out

$$\begin{cases} x = \left[\left(\cos\phi\cos\theta\sin\psi + \sin\phi\sin\psi \right) \sum_{i=1}^{4} F_i - k_{dtx}\dot{x} \right] m^{-1} \\ y = \left[\left(\cos\phi\sin\psi\sin\theta - \sin\phi\cos\psi \right) \sum_{i=1}^{4} F_i - k_{dty}\dot{y} \right] m^{-1} \\ z = \left[\left(\cos\phi\cos\theta \right) \sum_{i=1}^{4} F_i - k_{dtz}\dot{z} - mg \right] \end{cases} \tag{7}$$

Among them, $k_{dtx}, k_{dty}, k_{dtz}$ are the translational drag coefficients in the three directions of the X, Y, Z axis in the body coordinate system, respectively. Equation of Angular Motion The quadrotor performs not only linear motion, but also angular motion that rotates around the center of mass. According to the law of rigid body rotation

$$M = H\dot{} \tag{8}$$

Where $\mathbf{M}$ is the total external moment acting on the center of mass and $\mathbf{H}$ is the angular

Forest Chemicals Review
www.forestchemicalsreview.com
ISSN: 1520-0191
July-August 2022 Page No. 1592-1607
Article History: Received: 30 March 2022, Revised: 8 April 2022, Accepted: 15 April 2022, Publication: 30 April 2022

momentum. Check information available.

$$\dot{\mathrm{H}} = \left(\dot{\mathrm{H}}\right)_{\mathrm{r}} + \omega \times \mathrm{H} \tag{9}$$

Where $\mathbf{H}$ is represented as

$$\mathrm{H} = \begin{pmatrix} I_{xx}p - I_{xy}q - I_{xz}r \\ -I_{yx}p + I_{yy}\mathrm{q} - I_{yz}\mathrm{r} \\ -I_{zx}p - I_{zy}\mathrm{q} + I_{zz}\mathrm{r} \end{pmatrix} \tag{10}$$

In,

$$\mathrm{I} = \begin{pmatrix} I_{xx} & I_{\mathrm{xy}} & I_{xz} \\ I_{yx} & I_{yy} & I_{yz} \\ I_{zx} & I_{zy} & I_{zz} \end{pmatrix} \tag{11}$$

Where $\mathbf{I}$ represents the inertia tensor parameter. From the previous assumptions, it can be known that the quadrotor is a rigid body with uniform mass distribution and axisymmetric, so $I_{\mathrm{xy}} = I_{yx} = I_{yz} = I_{zy} = I_{xz} = I_{zx} = 0$, Equation (11) can be simplified as

$$\mathrm{I} = \begin{pmatrix} I_{xx} & 0 & 0 \\ 0 & I_{yy} & 0 \\ 0 & 0 & I_{zz} \end{pmatrix} \tag{12}$$

Among them, I_{xx} is the moment of inertia in the x-axis, I_{yy} is the moment of inertia in the y-axis, and I_{zz} is the moment of inertia in the z axis. Equation (10) can be simplified as

$$\mathrm{H} = \left(I_{xx}p, I_{yy}\mathrm{q}, I_{zz}\mathrm{r}\right)^{T} \tag{13}$$

In formula (9), $\left(\dot{\mathrm{H}}\right)_{\mathrm{r}}$ is expressed as

$$\left(\dot{\mathrm{H}}\right)_{\mathrm{r}} = \left(I_{xx}\dot{p}, I_{yy}\dot{q}, I_{zz}\dot{r}\right)^{T} \tag{14}$$

In formula (9), $\omega \times \mathbf{H}$ is expressed as

Forest Chemicals Review
www.forestchemicalsreview.com
ISSN: 1520-0191
July-August 2022 Page No. 1592-1607
Article History: Received: 30 March 2022, Revised: 8 April 2022, Accepted: 15 April 2022, Publication: 30 April 2022

$$\omega \times \mathrm{H} = \begin{pmatrix} (I_{zz} - I_{yy}) qr \\ (I_{xx} - I_{zz}) rp \\ (I_{yy} - I_{xx}) pq \end{pmatrix} \tag{15}$$

Among them, $(\dot{\mathbf{H}})_r$ is the rate of change of angular momentum in the body coordinate system and $\omega = (p, q, r)^T$ is the angular velocity in the body coordinate system. Substitute equations (14) and (15) into equation (9) to get

$$\dot{\mathrm{H}} = \begin{pmatrix} I_{xx}\dot{p} + (I_{zz} - I_{yy}) qr \\ I_{yy}\dot{q} + (I_{xx} - I_{zz}) pr \\ I_{zz}\dot{r} + (I_{yy} - I_{xx}) pq \end{pmatrix} \tag{16}$$

Substituting equation (16) into equation (8), we can get

$$\mathrm{M} = \begin{pmatrix} M_x \\ M_y \\ M_z \end{pmatrix} = \begin{pmatrix} I_{xx}\dot{p} + (I_{zz} - I_{yy}) qr \\ I_{yy}\dot{q} + (I_{xx} - I_{zz}) pr \\ I_{zz}\dot{r} + (I_{yy} - I_{xx}) pq \end{pmatrix} \tag{17}$$

Transforming formula (17), we get

$$\begin{pmatrix} \dot{p} \\ \dot{q} \\ \dot{r} \end{pmatrix} = \begin{pmatrix} \left[M_x - (I_{zz} - I_{yy}) qr \right] I_{xx}^{-1} \\ \left[M_y - (I_{xx} - I_{zz}) pr \right] I_{yy}^{-1} \\ \left[M_z - (I_{yy} - I_{xx}) pq \right] I_{zz}^{-1} \end{pmatrix} \tag{18}$$

According to Euler's theorem, the Euler angle (ϕ, θ, ψ) and the angular velocity $(p, q, r)^T$ in the body coordinate system have the following relationship

$$\begin{pmatrix} p \\ q \\ r \end{pmatrix} = \begin{pmatrix} 1 & 0 & -\sin\theta \\ 0 & \cos\phi & \sin\phi\cos\theta \\ 0 & -\sin\phi & \cos\phi\cos\theta \end{pmatrix} \begin{pmatrix} \dot{\phi} \\ \dot{\theta} \\ \dot{\psi} \end{pmatrix} \tag{19}$$

Can also be written as

Forest Chemicals Review
www.forestchemicalsreview.com
ISSN: 1520-0191
July-August 2022 Page No. 1592-1607
Article History: Received: 30 March 2022, Revised: 8 April 2022, Accepted: 15 April 2022, Publication: 30 April 2022

$$\begin{pmatrix} \phi \\ \theta \\ \psi \end{pmatrix} = \begin{pmatrix} p + p\sin\phi\tan\theta + r\cos\phi\tan\theta \\ q\cos\phi - r\sin\phi \\ q\sin\phi\sec\theta + r\cos\phi\sec\theta \end{pmatrix} \tag{20}$$

Derivating equation (20) to get

$$\begin{cases} \ddot{\phi} = \left[M_x - \dot{\theta}\dot{\psi}\left(I_{zz} - I_{yy} \right) \right] I_{xx}^{-1} \\ \ddot{\theta} = \left[M_y - \dot{\phi}\dot{\psi}\left(I_{xx} - I_{zz} \right) \right] I_{yy}^{-1} \\ \ddot{\psi} = \left[M_z - \dot{\phi}\dot{\theta}\left(I_{yy} - I_{xx} \right) \right] I_{zz}^{-1} \end{cases} \tag{21}$$

In order to decompose the nonlinear coupled model of the quadrotor into four independent control channels, the control input of the quadrotor can be defined as

$$\begin{pmatrix} U_1 \\ U_2 \\ U_3 \\ U_4 \end{pmatrix} = \begin{pmatrix} F_1 + F_2 + F_3 + F_4 \\ F_4 - F_2 \\ F_3 - F_1 \\ F_2 + F_4 - F_1 - F_2 \end{pmatrix} = \begin{pmatrix} k_t \sum_{i=1}^{4} \omega_i^2 \\ k_t \left(\omega_4^2 - \omega_2^2 \right) \\ k_t \left(\omega_3^2 - \omega_1^2 \right) \\ k_d \left(\omega_1^2 - \omega_2^2 + \omega_3^2 - \omega_4^2 \right) \end{pmatrix} \tag{22}$$

Among them, U_1 is the vertical lift control amount, U_2 is the roll motion control amount, U_3 is the pitch motion control amount, and U_4 is the yaw motion control amount.

IV. FLIGHT CONTROL METHOD FOR PATROLLING POINTS OF INTEREST ON HIGH-VOLTAGE TRANSMISSION TOWERS

4.1. Training samples

Let experienced staff operate and autonomous line patrol drones with the same hardware specifications, remote-controlled drones with the same hardware specifications to perform sampling flights for different towers according to the route, and synchronously record relevant data, including the real-time video recorded by the imager, and the real-time position of the aircraft , flight parameters such as attitude and speed, as well as information such as the model of the tower. For asymmetric towers, both sides should be trained and recorded separately [13]. Multiple training sessions are required for each type of tower, and the more training times, the more accurate the sample.

4.2. Data processing

Select and extract key information from the recorded data, including the motion trajectory of the point

Forest Chemicals Review
www.forestchemicalsreview.com
ISSN: 1520-0191
July-August 2022 Page No. 1592-1607
Article History: Received: 30 March 2022, Revised: 8 April 2022, Accepted: 15 April 2022, Publication: 30 April 2022

of interest captured from the flight video, and calculate the velocity increment in the movement, the relative position and relative trajectory of the UAV and the center of the given tower, etc., and Break down the flight process into action steps.

4.3. Information Fitting

A regression algorithm is used to fit the extracted information, and an appropriate fuzzy control algorithm is selected to form a preset controller. In addition to forming corresponding controllers for each type of tower, since the point of interest is mainly the insulator string, a general tower inspection controller can also be formed according to the tracking action of the decomposed insulator string; it is stipulated that the detection of the tower by the drone starts from the top, so The flight process of the drone finding and hovering near the first point of interest to be inspected from above the wire also needs to be fitted into the control algorithm and integrated into the general controller. Due to the complex flight environment, the distance between the fuselage and the tower, cables, obstacles and other entities must be constrained in real time during the actual flight [14]. The method of constraint is: use the focal length information of the imager to judge the distance in real time. When the distance between the UAV and some entities is less than the minimum safe distance and has not reached the position suitable for the observation point of interest, backtrack a distance according to the original route and use the The location of the entity is listed as a reference, and the approach is rerouted until the observation location is reached. If the number of backtracking reaches a certain number of times on the way to a certain point of interest, give up approaching the point of interest, hover over the point of interest to observe the point of interest before the last backtracking, and move to the next point of interest after backtracking.

V. SYSTEM CHECK

Based on the research and development of automatic inspection technology, a complete set of inspection equipment has been successfully developed, and the functional performance of the inspection system has been confirmed. At the same time, an intelligent diagnosis expert system has been developed, which can safely diagnose the status of transmission lines. The large-scale unmanned helicopter automatic inspection system has carried out the first actual live line inspection test in a certain section of the line, and has carried out all-round detection and diagnosis of the safe distance of the line channel, abnormal heating, abnormal discharge and equipment appearance and structural defects. Through the fine inspection flight, the ultraviolet discharge inspection was carried out on the lines and tower equipment in the inspection section [15]. No obvious discharge phenomenon was found, and the possibility of wire breakage was low. The inspection period is the non-contamination period, and the possibility of contamination of the insulator string is small. Through the channel inspection, it is found that there is soil erosion in the area near the tower foundation of the line channel, but it does not affect the safe operation of the line for the time being. Visible light inspection is carried out on the lines and tower equipment in the inspection section through fine inspection to check whether there are any abnormalities such as broken insulators, self-explosion, lack of displacement of anti-vibration hammers, foreign objects in tower wires, and corrosion of metal parts. It was found that the large side glass insulator string of the L1 phase of the No. 319 tower had a

Forest Chemicals Review
www.forestchemicalsreview.com
ISSN: 1520-0191
July-August 2022 Page No. 1592-1607
Article History: Received: 30 March 2022, Revised: 8 April 2022, Accepted: 15 April 2022, Publication: 30 April 2022

self-explosion phenomenon, as shown in Figure 4. Figure 5 shows the drop of the anti-vibration hammer on the large side conductor of the L3 phase of Tower 324 and the large side conductor of the L1 phase of Tower 327. There is a bird's nest on the L1 and L2 phases of Tower 319, but there is no possibility of being scattered to the conductor.

Fig.4 #319 Tower glass insulator self-exploding

Fig. 5 Line wire anti-vibration hammer falls off

The inspection results of this inspection have been fully verified by manual review and comparison with historical defect data. Some defects cannot be well determined by manual inspection observation, which shows the superiority of UAV inspection. The inspection shows that the automatic inspection technology has achieved the expected goal in the application of 220kV line inspection, and has a good inspection effect. 52 sorties of large-scale drone inspection tasks, the cumulative inspection line length is 230km, and the inspection mileage is 680km. A total of more than 200 hidden dangers of line defects were found, including more than 10 urgent and major defects. Distance drones were compared with manual measurements. This is the first time at home and abroad to use the large-scale unmanned helicopter inspection system, adopt the multi-sensor automatic inspection mode, and carry out the large-scale application of live line inspection in the actual operation of the power grid, accumulating valuable

Forest Chemicals Review
www.forestchemicalsreview.com
ISSN: 1520-0191
July-August 2022 Page No. 1592-1607
Article History: Received: 30 March 2022, Revised: 8 April 2022, Accepted: 15 April 2022, Publication: 30 April 2022

inspection experience.

TABLE 1 Comparison of UAV ranging and manual remeasurement results.

Location	UAV ranging/m	Manual retest/m	Obstacle Type
N40-41 gear	2.22	2.85	Tree barrier
N41-42 gear	3.99	3.80	low voltage line
N42-43 gear	4.18	4.20	low voltage line
N43-44 gear	3.90	4.40	low voltage line

VI. CONCLUSION

The 3D visualization system for transmission line corridors designed and implemented in this paper is based on the laser scanning data obtained by unmanned helicopters, and realizes the visualization of massive cloud data of laser points, visualization of terrain data, visualization of tower/transmission line models, and UAV flight process. 3D real-time visualization, designed and implemented a comprehensive UAV line patrol 3D visualization system platform. Aiming at the bottleneck problem that the machine memory cannot load all the 3D model data at one time, the dynamic data loading, efficient spatial indexing mechanism and dynamic model cutting algorithm are used to realize the true 3D visualization of massive scenes. Experiments show that the method can realize virtual reconstruction of 3D scene.

REFERENCES

[1]. Sui Yu, Ning Pingfan, Niu Pingjuan, et al. A review of research on the power inspection technology of mounted UAVs for overhead transmission lines. Power Grid Technology, Vol. 45(2021) No.9, p. 13-19.
[2]. Shao Guiwei, Liu Zhuang, Fu Jing, et al. Research progress of UAV inspection technology for overhead transmission lines. High Voltage Technology, Vol. 4(2020) No.1, p. 9-101.
[3]. Huang Zheng, Wang Yongqiang, Wang Hongxing, et al. UAV Smart Inspection System Based on Cloud-Mist Edge Heterogeneous Collaboration. China Electric Power, Vol. 53(2020) No.4, p. 18-24.
[4]. Chen Keyu, Shi Shushan. Application of an Infrared Image Enhancement Algorithm in UAV Inspection of Transmission Lines. Electronic Design Engineering, Vol. 28(2020) No.16, p. 57-62.
[5]. Liu Jierong, Wang Weiguan, He Qimiao, et al. UAV autonomous line patrol technology and system with leapfrog charging (2): automatic charging control based on machine vision. Journal of Electric Power Science and Technology, Vol. 36(2021) No.6, p. 79- 82.
[6]. Tang Hongliang, Zhou Rongliang, Yang Minkun, et al. Automatic measurement technology of transmission lines based on UAV inspection. Electronic Measurement Technology, Vol. 43(2020) No.5, p. 95-101.
[7]. Li Ning, Li Bo, Chen Wei, et al. Design of high-performance power integrated inspection system based on multi-rotor UAV platform. Electronic Design Engineering, Vol. 29(2021) No.24, p. 59-62.
[8]. Tao Xiongjun, Ruan Jun, Wang Anjun. A Semantic Interaction Method for UAV Navigation in Transmission Line Inspection. Computer System Applications, Vol. 29(2020) No.9, p. 77-81.

Forest Chemicals Review
www.forestchemicalsreview.com
ISSN: 1520-0191
July-August 2022 Page No. 1592-1607
Article History: Received: 30 March 2022, Revised: 8 April 2022, Accepted: 15 April 2022, Publication: 30 April 2022

[9]. Gao Yisong, Chen Weizhuo, Wang Ji, et al. Inspection of UAV Transmission Line Construction Vehicles under Android Platform. Computer System Applications, Vol. 29(2020) No.2, p. 59-62.

[10]. Guan Jiahua, Sun Guanghui, Lu Kaiye, et al. Leapfrog charging UAV autonomous line patrol technology and system (1): GPS/RTK-based UAV autonomous positioning. Journal of Electric Power Science and Technology, Vol. 36(2021) No.5, p. 66-71.

[11]. Li Junpeng, Zhang Jiwei, Yu Yanwen. Research on intelligent ground monitoring system based on inspection drones in power grid industry. Information Technology, Vol. 44(2020) No.6, p. 59-62.

[12]. Jiang Liang, Zheng Enhui, Tong Jingzhe. Design of UAV relocation camera system based on power tower inspection. Science and Technology Bulletin, Vol. 4(2020) No.10, p.46-54.

[13]. Lin Huozheng, Chen Jie, Shen Bin, et al. Design of emergency charging power management system for inspection drones. Journal of Fuzhou University: Natural Science Edition, Vol. 48(2020) No.2, p.71-74.

[14]. Yuan Linfeng, Kodak, Xu Chao, et al. Research on Autonomous Obstacle Avoidance System of Power Inspection UAV Based on Orthogonal Lidar. Automation Technology and Application, Vol. 40(2021) No.7, p. 59-62.

[15]. Yang Hao, Lin Nan, Yuan Chen, et al. Information security risk analysis and protection of UAVs for power line patrolling. Journal of Electric Power Science and Technology,36(2021) No.4, p. 99-104.